HHS Public Access

Author manuscript

Cell Rep. Author manuscript; available in PMC 2017 November 01.

Published in final edited form as:

Cell Rep. 2017 August 15; 20(7): 1533–1542. doi:10.1016/j.celrep.2017.07.051.

microRNA-9 couples brain neurogenesis and angiogenesis

Romain Madelaine[1], **Steven A. Sloan**[2], **Nina Huber**[1], **James H. Notwell**[3], **Louis C. Leung**[1], **Gemini Skariah**[1], **Caroline Halluin**[1], **Sergiu P. Paşca**[1], **Gill Bejerano**[3,4], **Mark A. Krasnow**[5], **Ben A. Barres**[2], and **Philippe Mourrain**[1,6,7,*]

[1]Stanford Center for Sleep Sciences and Medicine, Department of Psychiatry and Behavioral Sciences, Stanford, CA 94305, USA

[2]Department of Neurobiology, Stanford, CA 94305, USA

[3]Department of Computer Science, Stanford, CA 94305, USA

[4]Department of Developmental Biology, Stanford, CA 94305, USA

[5]HHMI and Department of Biochemistry, Stanford, CA 94305, USA

[6]INSERM 1024, Ecole Normale Supérieure Paris, 75005, France

SUMMARY

In the developing brain, neurons expressing VEGF-A and blood vessels grow in close apposition, but many of the molecular pathways regulating neuronal VEGF-A and neurovascular system development remains to be deciphered. Here, we show that miR-9 links neurogenesis and angiogenesis through the formation of neurons expressing VEGF-A. We found that miR-9 directly targets the transcription factors TLX and ONECUTs to regulate *VEGF-A* expression. miR-9 inhibition leads to increased TLX and ONECUT expression resulting in *VEGF-A* overexpression. This untimely increase of neuronal VEGF-A signal leads to the thickening of blood vessels at the expense of the normal formation of the neurovascular network in the brain and retina. Thus, this conserved transcriptional cascade is critical for proper brain development in vertebrates. Because of this dual role on neural stem cell proliferation and angiogenesis, miR-9 and its downstream targets are promising factors for cellular regenerative therapy following stroke and for brain tumor treatment.

eTOC blurb

[*]Correspondence: mourrain@stanford.edu.
[7]Lead Contact

AUTHORS CONTRIBUTIONS

R.M. and P.M. designed and analyzed *in vivo* experiments. R.M. performed *in vivo* experiments with the assistance of G.S. and C.H.. L.C.L. established *Tg(gfap:gal4)* line. S.A.S., N.H., R.M., S.P.P., B.A.B. and P.M. designed and analyzed *in vitro* experiments. S.A.S and N.H. performed *in vitro* experiments. J.H.N. and G.B. performed *in silico* analysis. M.A.K. advised on the blood vessel study. R.M., S.A.S., J.H.N., G.B., B.A.B. and P.M wrote the manuscript. PM supervised the entire work.

Competing financial interests: the authors declare no competing financial interests.

The coordination of neuronal and vascular cells development is critical to ensure the proper formation of the vertebrate brain. Madelaine et al. show that the microRNA-9 couples neurogenesis and brain angiogenesis through the inhibition of Tlx and Onecut transcription factors regulating neuronal VEGF-A expression.

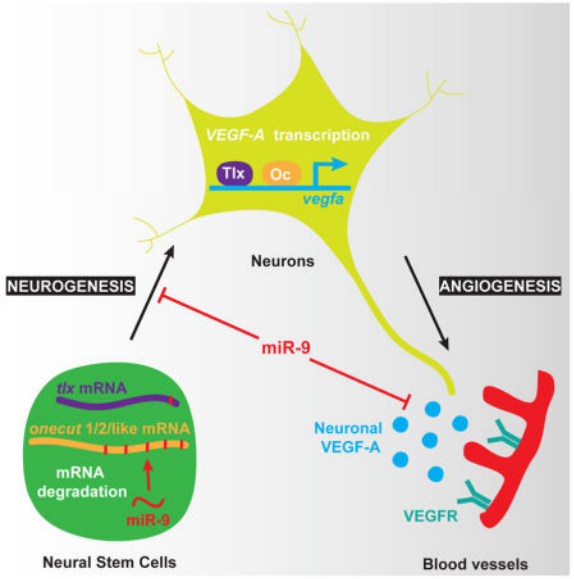

INTRODUCTION

The development of the neurovascular system is essential to ensure proper functioning of the central nervous system (CNS). The vertebrate CNS is predominantly vascularized through the process of angiogenesis, in which proliferating endothelial cells (ECs) form new vessels by sprouting from a pre-existing vascular network (Risau, 1997). Studies across vertebrates have identified many of the conserved cellular and molecular mechanisms underlying CNS vascularization (Gerhardt et al., 2003; Ruhrberg et al., 2002; Stone et al., 1995). To date, the most potent angiogenic intercellular signal identified is the vascular endothelial growth factor VEGF-A (Ferrara and Kerbel, 2005; Ruhrberg and Bautch, 2013). VEGF-A gradients guide the ingression and growth of blood vessels within neural tissues (Ruhrberg et al., 2002). During development, VEGF-A is also involved in many aspects of vasculature formation including sprouting, pruning, connectivity, vessel caliber, and survival (Ruhrberg and Bautch, 2013).

Current models of CNS angiogenesis and neurovascular development are largely glia-centric (Armulik et al., 2010; Bozoyan et al., 2012; Daneman et al., 2010), despite the observation that VEGF-A is expressed in the brain prior to the generation of mature astrocytes during early development (Breier et al., 1992; Walchli et al., 2015). Importantly, it was also shown that astrocyte-derived VEGF-A is dispensable to retinal vasculature formation (Scott et al., 2010), suggesting a critical role for neuronal VEGF-A in retinal angiogenesis. Consistent with a neuronal function during neurovascular development in the CNS, VEGF-A expression has been observed in multiple types of neurons in different species (D'Amore, 2007; Gerhardinger et al., 1998; Ogunshola et al., 2002; Shima et al., 1996). Further, a

functional neuronal contribution has been suggested in the peripheral nervous system, where nerve-derived VEGF can induce arteriogenesis (Mukouyama et al., 2002). However, the exact cell type regulating this process was unclear as both Schwann cells and sensory neurons forming the peripheral nerve express VEGF. In the spinal cord, one recent report has shown that VEGF-A derived from neurons is required for vascularization (Wild et al., 2017). Despite these observations, how neuronal VEGF-A is regulated and contributes to the formation of the blood vessel network throughout the developing brain remain poorly understood.

In this study, we investigate the coupling role of *microRNA-9* (*miR-9*) activity to neurogenesis and angiogenesis during brain development. *miR-9* expression is detected in neural stem cells (NSCs) (Coolen et al., 2013) and its inhibition transiently increases proliferation, reducing the number of early-born neurons while increasing the number of late-differentiating neurons (Bonev et al., 2011; Coolen et al., 2012; Shibata et al., 2011). Interestingly, miR-9 has also been associated to cancer cell vascularization *in vitro* (Zhang et al., 2012; Zhuang et al., 2012), suggesting a potential role for this microRNA in physiological angiogenesis *in vivo*. However, direct evidence has been lacking. Here, we identify a key transcriptional cascade downstream of miR-9 that regulates neuronally-derived VEGF-A. Our results uncover a delicate balance of VEGF-A signaling that controls blood vessel formation, carefully maintained by miR-9 negative regulation of *TLX* and *ONECUT* expression. This study indicates that miR-9-dependent neuronal expression of VEGF-A is a main component of neurovascular system development in the vertebrate brain.

RESULTS

VEGF-A is highly expressed in neurons before astrogenesis in the developing human brain

To study early neuronal VEGF-A expression and function, we first investigated the expression pattern of VEGF-A in the developing human brain. We examined cortical neurons purified from 14 gestational week (14GW) fetal tissue (Fig. 1A). At this age of human fetal cortical development, gliogenesis has not yet begun and the $GFAP^+$ cells represent young neural stem cells (Zhang et al., 2016). We observed robust VEGF-A expression in primary cultures of 14GW human fetal cortical neurons (Fig. 1A′, B; 98.5%, n=201) but also in iPSC-derived neurons (Fig. 1C), suggesting that VEGF-A is a hallmark of young neurons and that neuronally-derived VEGF-A may have a function during developmental processes. We then extended this mammalian observation to the developing zebrafish. We focused on the hindbrain and retina, two brain structures used as archetype regions for brain vasculature development (Gerhardt et al., 2003; Ruhrberg et al., 2002). We found that during early zebrafish development (2 day-old), VEGF-A is expressed in neurons throughout the CNS (retina and hindbrain in Fig. 1D and Fig. S1A respectively, and spinal cord in (Wild et al., 2017)). Consistent with a role for neuronally-derived VEGF-A in angiogenesis, we found that the neurovasculature is embedded or in close cellular proximity with axons (Fig. S1B–H′). Together with the axonal expression of VEGF-A observed in cultured primary and iPSC-derived neurons (Fig. 1B, C), this observation suggested a possible neuronal influence in vascular morphogenesis. Thus, we hypothesized that

neuronally-derived VEGF-A is a component of the neurovascular system formation from fish to human.

VEGF-A expression is regulated by miR-9 in the brain

We reasoned that miR-9 may control vasculature development by modulating the neuronal expression of VEGF-A. Using human iPSC-derived cortical spheroids (Fig. 1E), which are 3D cultures resembling the developing human cerebral cortex (Pasca et al., 2015), we identified *MIR-9* expression in NSCs in the *SOX2*$^{+}$ proliferative zones of the developing human nervous tissue (Fig. 1E′ and E″). Using neural stem cells markers (Chapouton et al., 2010; Coolen et al., 2012; Schmidt et al., 2013), we also confirmed *miR-9* expression in *gfap*$^{+}$ and *deltaA*$^{+}$ NSCs in the zebrafish brain (Fig. S2A, B), and uncovered a novel *miR-9* expression in the Müller cells (GS^{+}), the neural stem cells of the retina (Fig. 1F). Because of the conservation of *miR-9* expression in the human and zebrafish developing brains, and its well-known function in neurogenesis, we hypothesized that miR-9 may be an important regulator of neuronal VEGF-A expression.

We next investigated how the expression of VEGF-A might be affected by miR-9 using both miR-9 depletion and miR-9 mimics to decrease and increase miR-9 activity, respectively (Fig. 2A). Because of the miR-9 gene duplication (7 genes in teleosts and 3 genes in mammals), genetic manipulation of this microRNA is not simple. Fortunately, all miR-9 genes produce an identical mature 23bp sequence that can be targeted by a single antisense miR-9 morpholino (MO; (Bonev et al., 2011; Coolen et al., 2012)). We found that *vegfa* mRNA accumulation was strongly increased throughout the brain including retina in the miR-9 depleted larvae, while reduced in miR-9 mimics injected larvae (Fig. 2B). These observations suggest that miR-9 controls directly or indirectly VEGF-A expression during neurovascular development, and can potentially regulate blood vessels formation in the brain.

Brain and retinal blood vessel networks are disorganized in absence of miR-9

The onset of *miR-9* expression in the hindbrain and retina during the second day of zebrafish development is consistent with the formation of the vasculature in these regions (Fig. S1B, D and Fig. S2C). To investigate the potential coupling of miR-9 activity to neurogenesis and neurovascular development, we inhibited all *miR-9* genes (Fig. S3A) in a *kdrl/vegfr2:mCherry* transgenic line that labels the entire vasculature (Chi et al., 2008). While the vascular organization outside of the CNS was normal (Fig. S3B), many aspects of the blood vessel network were affected in the brain and retina when miR-9 activity was impeded (Fig. 2C, D and Fig. S3C). In the brain, the middle mesencephalic central arteries (MMCtA) were affected in the midbrain, as well as the central arteries (CtA) in the hindbrain. Similarly, in the retina, the hyaloid vasculature was strongly reduced, but the remaining vessels were thicker. These results suggest a role for miR-9 in brain and retina angiogenesis starting on the second day of development.

As a post-transcriptional regulator, we reasoned that miR-9 may have a dose-dependent effect on brain angiogenesis. In the eye, as the level of miR-9 knockdown decreased, the hyaloid vasculature progressively recovered its mesh-like organization and retinal vessel

network cupping the lens (Fig. S3D, F). In the zebrafish hindbrain, the Central Arteries (CtAs) sprout from the Primordial Hindbrain Channels (PHBCs) at 32 hpf (Ulrich et al., 2011), an event concomitant with the onset of miR-9 expression (Coolen et al., 2012). While Posterior Communicating Segments (PCS) and the Basilar Artery (BA) were unaffected in miR-9 morphants, CtAs failed to develop normally (Fig. 2C, D). When they did sprout, CtAs were shorter and/or thinner, displayed multidirectional filopodial extensions and failed to reach the midline. In contrast to CtAs, PHBCs appeared to be thicker (Fig. 2C–F), and showed an increase diameter when miR-9 was depleted (Fig. 2F; 11.1 ±1.3 μm vs. 15.2 ±3.2 μm in control and miR-9 morphant, respectively). Furthermore, when miR-9 expression was abolished, we observed an increased number of ECs in PHBCs (22.8 ±2.7 vs. 32.3 ±6.2 in control and miR-9 morphant, respectively) correlated to a 34% decrease in CtAs sprouting (Fig. 2E–G), suggesting that ECs prematurely differentiated in the PHBCs and/or that their capacity to be recruited to form CtAs was affected. As miR-9 expression was restored, the sprouting of CtAs was progressively recovered (Fig. 2G and Fig. S3E). These observations are consistent with the previous demonstration that EC migration from PHBCs is the primary mechanism of CtAs formation (Ulrich et al., 2011). Altogether, these results indicate that the level of miR-9 activity regulates the formation of the neurovascular system in the brain.

miR-9 limits VEGF-A signaling to regulate blood vessels development

We next hypothesized that VEGF abnormal expression induces the thickening of already formed PHBCs at the expense of the normal formation of CtAs. To test this hypothesis, we used a conditional approach to counteract the excess of VEGF-A signal with SU5416, a specific inhibitor of the VEGF-Receptor (VEGFR). SU5416 was added in the fish water at 30 hpf, at a very low dose compared to what is used normally to study VEGFR function (Ulrich et al., 2011), 1 μM vs. 0.06 μM in our experiment). We chose the lowest dose leading to a vasculature defect to validate that the VEGF signal was at least partially impaired (Fig. 2H, I). We observed that a moderate inhibition of the VEGF signal in the miR-9 depleted larvae at the onset of CtAs angiogenesis (SU5416 0.06 μM from 30 hpf to 72 hpf) efficiently rescued the large majority of the blood vessel network (Fig. 2H, I; 86% versus 67% with the miR-9 MO only, compared to 100% in control morphant). This result shows that miR-9 directly or indirectly limits VEGF-A/VEGFR signal which in turn controls normal sprouting of new blood vessels from the preexisting vascular network.

TLX and ONECUTs are conserved direct targets of miR-9 *in vivo*

Because we found that no VEGF ligand genes harbor miR-9 target sites in their 3′UTR, we utilized a computational approach (Bartel, 2009) to identify targets of miR-9 acting upstream of *VEGF-A*. We identified a number of gene expression regulators that contain miR-9 target sites and that were conserved from human to zebrafish: *ONECUT1*, *ONECUT2*, *LIN28*, *FOXP1*, *FOXP2*, *FOXP4,* and *TLX/NR2E1*. Among these candidates, only *tlx/nr2e1, onecut1, onecut2* and *onecut-like* (human *OC2* orthologue in zebrafish) mRNA expression levels demonstrated miR-9 dependence *in vivo* (Fig. S4A–D). *tlx* and *onecut1* 3′UTRs each bear a single miR-9 target site that we validated *in vivo* by using target protection experiments (TP) and fluorescent sensor assays (Fig. 3A–C and Fig. S4E; (Zhao et al., 2009)). In the case of *onecut2* and *onecut-like*, we identified 12 and 5 potential

miR-9 binding sites in their respective 3′UTRs (Fig. 3D and Fig. S4D). In the presence of miR-9 mimics, we observed a 56% decrease in EGFP expression fused to the 3′UTR of *onecut-like* (Fig. S4F). Finally, using target protection we validated the direct interaction with one miR-9 site particularly conserved between *ONECUT2* orthologues across vertebrates, and between *onecut2* and *onecut-like* paralogues in zebrafish (Fig. 3A, D). Our results demonstrate *in vivo* that *tlx* and *onecut* transcription factor mRNAs are direct conserved targets of miR-9 in the vertebrate brain.

TLX and ONECUT regulate *VEGF-A* transcriptional expression *in vivo*

Because human and zebrafish *VEGF-A* promoters carry putative TLX and ONECUT binding sites, we next investigated the capacity of these transcription factors to mediate the miR-9-dependent effect on *vegfa* expression. In zebrafish gastrulae, we expressed *tlx* and *onecut* ORFs under the control of a heat-shock promoter. We assessed their impact on the expression of endogenous *vegfa* or an e*gfp* reporter driven by a compact *vegfa* promoter (Fig. 3E). After heat-shock, we observed widespread expression of *vegfa* and *egfp* transcripts. These results indicated that both Tlx and Onecut are sufficient to induce endogenous *vegfa* and exogenous *egfp* transcription *in vivo* (Fig. 3F–H). We next verified using a *huc* staining that no neurons were formed following Tlx or Onecut expression, demonstrating that *vegfa* transcription is induced independently of the acquisition of a neuronal fate. We then performed a similar set of experiments where a p2A-EGFP cleavable reporter was fused to Tlx and Oc proteins to determine the cell autonomous transcriptional activation of the *vefga* gene. We observed co-localization of *vegfa* mRNA with EGFP in as little as 15 min after a 15 min heat-shock, demonstrating fast cell autonomous transcriptional activation of *vegfa* by Tlx and Oc (Fig. 3I). We then inhibited Tlx and Oc expression in miR-9 depleted embryos and observed a reduced induction of *vegfa* expression (Fig. 3J), further supporting Tlx and Oc endogenous roles downstream of miR-9 and upstream of *vegfa* expression.

TLX and ONECUT promote the differentiation of neurons expressing VEGF-A

TLX and OC expression can be detected in NSCs and neurons ((Sapkota et al., 2014; Shi et al., 2004; Yuan et al., 2015; Zhang et al., 2016); www.brainrnaseq.org) and we showed in zebrafish that their expression in NSCs is strongly reduced when miR-9 is robustly expressed in these cells (Fig. S5). These observations suggested a role for these transcription factors in NSCs differentiation into neurons across vertebrates. First, we studied the role of these transcription factors using primary human fetal neural stem cells at 14GW, a stage where no differentiated astrocytes are present in the human brain. We transfected purified hENSCs with plasmids for EGFP, TLX-p2A-EGFP, or OC2-p2A-EGFP, and allowed them to differentiate in culture for one week. For TLX-p2A-EGFP and OC2-p2A-EGFP transfected cells, we observed that the NSC pool was substantially depleted (Fig. S6A; 0.8% and 2.4% respectively, versus 15.2% in the control). Interestingly, this reduction of ~90% in the number of NSCs is not correlated to a reduction in the number of $TUJ1^+$ cells, but to a 9% increase of neurons expressing VEGF-A (Fig. S6A, B). Because of the limited access to human fetal tissue, we next investigated the capacity of the miR-9/Tlx/Oc cascade to control neurogenesis in zebrafish. Similarly to human cell culture observation, miR-9 depletion in zebrafish dramatically decreases the pool of NSCs in both brain and retina while increasing

deltaA^{+} and *ascl1a*$^{+}$ neural progenitors, and *huc*$^{+}$ neurons (Fig. S6C, D), as previously described (Coolen et al., 2012). We also observed that Tlx or Ocl expression in zebrafish NSCs reduces GS expression and that when *tlx* and *ocl* mRNAs are preserved from miR-9-induced decay, *deltaA*$^{+}$ neural progenitors are increased in the developing brain (Fig. S6C, D). Together, these results validate the neurogenic function of TLX and OC downstream of miR-9, and suggest that embryonic NSCs depletion results from a transition into neuronal fates, promoting the differentiation of neurons expressing VEGF-A.

Neuronal expression of VEGF-A induced by TLX and ONECUT controls brain vascular development

To test whether TLX/OC-dependent VEGF-A expression controls vascular formation in the developing CNS, we expressed these transcription factors under the control of a neuronal promoter (using *Tg(alpha-tubulin:gal4)* line and the GAL4/UAS system) and also used target protection to stabilize endogenous Tlx and Oc mRNAs. In both experiments, Tlx or Oc exogenous and endogenous expression induced *vegfa* upregulation, associated to a reduction of CtAs sprouting (Fig. 4A–D and Fig. S7). We also observed an additive impact of Tlx and Oc on *vegfa* expression and angiogenesis defects. These results provide *in vivo* evidence that miR-9 can control neurovascular development by directly inhibiting *tlx* and *onecut* expression and repressing the VEGF-A pathway.

Finally, to further validate that TLX and OC effects on neurovascular development are mediated through neuronal VEGF-A expression, we expressed VEGF-A in neurons using the *alpha-tubulin:gal4* transgenic line. Consistent with the pro-angiogenic role of VEGF-A, we showed that overexpression of *vegfa* in neurons led to a global hyperplasia of blood vessels in the brain (Fig. 4E), but some vessels like MMCtAs in the midbrain are missing (Fig. 4E′). In the hindbrain, we observed a 54% decreases in CtAs sprouting while PHBCs appears thicker (Fig. 4E″ and F). Similarly, in the retina, the development of the hyaloid vasculature is affected and retinal vessels are largely missing (Fig. 4E and E′). Thus, the effect of *vegfa* neuronal expression on blood vessels development was reminiscent of the miR-9 depletion phenotype. This observation suggests that the increase angiogenesis from the preexisting vascular network affects the availability/capability of ECs to form subsequent new blood vessels during development. Overall these results uncover a conserved miR-9-dependent cascade regulating VEGF-A expression (Fig. 4G), and indicate that neuronally-derived VEGF-A is a critical angiogenic factor in the developing vertebrate brain.

DISCUSSION

Neuronal VEGF-A is an angiogenic factor during early brain development in human

Consistent with a neuronal role in angiogenesis in the developing human brain, our data show that neuronally-derived VEGF-A is highly expressed by human fetal primary neurons at a time when no differentiated astrocytes are detected (14 gestational weeks in human fetal cortices). This may represent the major source of VEGF-A necessary for neurovasculature formation during early development. In comparison to radial glia, cortical neurons display a much weaker immunostaining for VEGF-A proteins, but because neurons are much more abundant during early CNS development, the gross VEGF signal produced by these cells

may be entirely sufficient for normal vascularization. Our data showing that iPSC derived neurons within human cortical spheroids (which are not vascularized) express VEGF-A indicates that neuronal VEGF-A expression is a part of the genetic program controlling neuronal identity, and is not solely a response to angiogenic processes. Interestingly, in both primary neurons and iPSC derived neurons we detected a dual localization of VEGF-A in the nucleus and in vesicular structures of the cytoplasm, suggesting that in addition to its *trans* activity through VEGF Receptor-2 activation, VEGF-A may also have unappreciated biological functions, such as transcriptional control of gene expression via a cell autonomous mechanism, as demonstrated for VEGF-D in human lung fibroblasts (El-Chemaly et al., 2014).

miR-9 is a critical factor coupling neurogenesis and angiogenesis

The coordination of neurogenesis and angiogenesis is critical to the proper formation of the vertebrate brain and the control of VEGF-A expression by the neurogenesis modulator miR-9 reveals a conserved transcriptional cascade linking neuronal and vascular development. Two previous studies have reported a link between miR-9 and tumor angiogenesis *in vitro*, but the physiological significance of the reported mechanisms was unclear because these reports produced paradoxical results: showing a pro-angiogenic activity of miR-9 via the JAK-STAT pathway in one case (Zhuang et al., 2012) and an anti-angiogenic activity via matrix metalloproteinase 14 in the other (Zhang et al., 2012). Here, we demonstrated that miR-9 is regulating angiogenesis *in vivo* by decreasing the stability of *tlx* and *onecut* mRNAs to limit neuronal VEGF-A signaling. The constitutive neuronal expression of both Tlx and Oc using a neuronal driver led to vasculature defects similarly to neuronal *VEGF-A* expression, demonstrating their capacities to control *VEGF-A* transcription in neurons downstream of miR-9 to regulate brain and retina angiogenesis. These findings are not only significant for our understanding of the early vascularization in the CNS but also as targets for anti-VEFG therapies in retinal diseases and brain tumors.

EXPERIMENTAL PROCEDURES

Fish developmental conditions and immunostaining

Embryos were raised and staged according to standard protocols (Kimmel et al., 1995). Our animal protocol (#9935) is approved by the American Association for the Accreditation of Laboratory Animal Care (AAALAC), in accordance with Stanford University animal care guidelines. Embryos were fixed overnight at 4°C in 4% PFA, after which they were dehydrated in ethanol. Immunostainings were performed using either anti-GFP (1/1000, Torrey Pines Biolabs), anti-HuC/D (1/500, Molecular Probes), anti-DsRed (1/500, Clontech), anti-GS (1/500, Fischer) and anti-Acetylated Tubulin (1/500, Sigma) as primary antibodies and Alexa 488 or Alexa 555-conjugated goat anti-rabbit IgG or goat anti-mouse IgG (1/1000) as secondary antibodies (Molecular Probes).

Primary human embryonic neural stem cells immunostaining

Purified neural stem cells were obtained from 14 week-old human fetal brains (IRB approval under Protocol #20083). For immunostaining, coverslips were fixed in 4% PFA for 10 minutes before blocking with 10% goat serum and 0.1% TritonX for 30 minutes. The

primary antibodies include GFAP (1/1500, DAKO), Tuj1 (1/1500, Covance), VEGF-A (1/50, Santa Cruz), and GFP (1/1000, Abcam). Coverslips were incubated with primary antibody overnight in blocking solution, washed in PBS, and then incubated with secondary antibodies (Alexa) in blocking solution for 90 minutes prior to mounting.

Human iPSC-derived cortical neurons immunostaining

Human cortical spheroids (hCSs) were generated from human iPSC as previously described (Pasca et al., 2015). The generation of iPSCs were approved by the Stanford IRB. Fibroblasts for reprogramming were collected and deidentified following informed consent. For immunostaining, the samples were fixed in 4% PFA for 10 minutes before blocking with 10% goat serum and 0.3% Triton-X100 for one hour. Samples were incubated with primary antibodies (anti-VEGF-A; 1/100, Santa Cruz), anti-HuC/D (1/400, Life technology), anti-MAP2 (1/1500, Synaptic Systems) in 10% goat serum for 2 hours, washed with PBS and incubated with secondary antibodies (Alexa-conjugated, Life technology) in 10% goat serum for 45 minutes prior to mounting.

Image acquisition cell counting and blood vessel quantification

Confocal images were acquired using a Leica SP5 confocal microscope or a Leica TCS SP8 confocal microscope (Stanford cell science imaging facility). Images were prepared using Photoshop (Adobe) and for cell counting and blood vessel quantification confocal, stacks were analysed using ImageJ software. Statistical analyses associated with each figure are reported in the figure legends.

Supplementary Material

Refer to Web version on PubMed Central for supplementary material.

Acknowledgments

We thank members of the Mourrain, Barres and Bejerano laboratories for insightful discussions. We are grateful to Drs. Pamela A. Raymond, Neil C. Chi, David Traver, Holger Knaut, Maximiliano L. Suster, William S. Talbot, Thomas S. Becker and Nathan Lawson for gift of reagents or helpful discussions. We would also like to thank the Stanford CSIF Imaging platform.

FUNDING

This work was supported by grants from the National Institute of Health: P.M. (NS062798, DK090065 and MH099647), G.B (HG005058), S.A.S. (F30MH106261 and T32GM007365) and B.A.B. (MH099555-03). P.M. was also supported by the BrightFocus Foundation, R.M. by EMBO Long Term Fellowship (ALTF 413-2012) and the BrightFocus Foundation, J.H.N. by National Science Foundation Fellowship (DGE-1147470) and a Bio-X Stanford Interdisciplinary Graduate Fellowship, S.A.S by a Bio-X-Stanford Predoctoral Fellowship, G.B by a Packard Fellowship, N.H. by Dean's Postdoctoral Fellowship and Child Health Research Institute Postdoctoral Fellowship UL1-TR001085, S.P.P. by the NIMH BRAINS Award (R01MH107800), the MQ Fellow Award, Donald E. and Delia B. Baxter Foundation Award, the Kwan Foundation.

References

Armulik A, Genove G, Mae M, Nisancioglu MH, Wallgard E, Niaudet C, He L, Norlin J, Lindblom P, Strittmatter K, et al. Pericytes regulate the blood-brain barrier. Nature. 2010; 468:557–561. [PubMed: 20944627]

Bartel DP. MicroRNAs: target recognition and regulatory functions. Cell. 2009; 136:215–233. [PubMed: 19167326]

Bonev B, Pisco A, Papalopulu N. MicroRNA-9 reveals regional diversity of neural progenitors along the anterior-posterior axis. Developmental cell. 2011; 20:19–32. [PubMed: 21238922]

Bozoyan L, Khlghatyan J, Saghatelyan A. Astrocytes control the development of the migration-promoting vasculature scaffold in the postnatal brain via VEGF signaling. The Journal of neuroscience: the official journal of the Society for Neuroscience. 2012; 32:1687–1704. [PubMed: 22302810]

Breier G, Albrecht U, Sterrer S, Risau W. Expression of vascular endothelial growth factor during embryonic angiogenesis and endothelial cell differentiation. Development. 1992; 114:521–532. [PubMed: 1592003]

Chapouton P, Skupien P, Hesl B, Coolen M, Moore JC, Madelaine R, Kremmer E, Faus-Kessler T, Blader P, Lawson ND, et al. Notch activity levels control the balance between quiescence and recruitment of adult neural stem cells. The Journal of neuroscience: the official journal of the Society for Neuroscience. 2010; 30:7961–7974. [PubMed: 20534844]

Chi NC, Shaw RM, De Val S, Kang G, Jan LY, Black BL, Stainier DY. Foxn4 directly regulates tbx2b expression and atrioventricular canal formation. Genes & development. 2008; 22:734–739. [PubMed: 18347092]

Coolen M, Katz S, Bally-Cuif L. miR-9: a versatile regulator of neurogenesis. Frontiers in cellular neuroscience. 2013; 7:220. [PubMed: 24312010]

Coolen M, Thieffry D, Drivenes O, Becker TS, Bally-Cuif L. miR-9 controls the timing of neurogenesis through the direct inhibition of antagonistic factors. Developmental cell. 2012; 22:1052–1064. [PubMed: 22595676]

D'Amore PA. Vascular endothelial cell growth factor-a: not just for endothelial cells anymore. The American journal of pathology. 2007; 171:14–18. [PubMed: 17591949]

Daneman R, Zhou L, Kebede AA, Barres BA. Pericytes are required for blood-brain barrier integrity during embryogenesis. Nature. 2010; 468:562–566. [PubMed: 20944625]

El-Chemaly S, Pacheco-Rodriguez G, Malide D, Meza-Carmen V, Kato J, Cui Y, Padilla PI, Samidurai A, Gochuico BR, Moss J. Nuclear localization of vascular endothelial growth factor-D and regulation of c-Myc-dependent transcripts in human lung fibroblasts. American journal of respiratory cell and molecular biology. 2014; 51:34–42. [PubMed: 24450584]

Ferrara N, Kerbel RS. Angiogenesis as a therapeutic target. Nature. 2005; 438:967–974. [PubMed: 16355214]

Gerhardinger C, Brown LF, Roy S, Mizutani M, Zucker CL, Lorenzi M. Expression of vascular endothelial growth factor in the human retina and in nonproliferative diabetic retinopathy. The American journal of pathology. 1998; 152:1453–1462. [PubMed: 9626050]

Gerhardt H, Golding M, Fruttiger M, Ruhrberg C, Lundkvist A, Abramsson A, Jeltsch M, Mitchell C, Alitalo K, Shima D, et al. VEGF guides angiogenic sprouting utilizing endothelial tip cell filopodia. The Journal of cell biology. 2003; 161:1163–1177. [PubMed: 12810700]

Kimmel CB, Ballard WW, Kimmel SR, Ullmann B, Schilling TF. Stages of embryonic development of the zebrafish. Developmental dynamics: an official publication of the American Association of Anatomists. 1995; 203:253–310. [PubMed: 8589427]

Lannoy VJ, Burglin TR, Rousseau GG, Lemaigre FP. Isoforms of hepatocyte nuclear factor-6 differ in DNA-binding properties, contain a bifunctional homeodomain, and define the new ONECUT class of homeodomain proteins. The Journal of biological chemistry. 1998; 273:13552–13562. [PubMed: 9593691]

Mukouyama YS, Shin D, Britsch S, Taniguchi M, Anderson DJ. Sensory nerves determine the pattern of arterial differentiation and blood vessel branching in the skin. Cell. 2002; 109:693–705. [PubMed: 12086669]

Ogunshola OO, Antic A, Donoghue MJ, Fan SY, Kim H, Stewart WB, Madri JA, Ment LR. Paracrine and autocrine functions of neuronal vascular endothelial growth factor (VEGF) in the central nervous system. The Journal of biological chemistry. 2002; 277:11410–11415. [PubMed: 11777931]

Pasca AM, Sloan SA, Clarke LE, Tian Y, Makinson CD, Huber N, Kim CH, Park JY, O'Rourke NA, Nguyen KD, et al. Functional cortical neurons and astrocytes from human pluripotent stem cells in 3D culture. Nature methods. 2015; 12:671–678. [PubMed: 26005811]

Plaisance V, Abderrahmani A, Perret-Menoud V, Jacquemin P, Lemaigre F, Regazzi R. MicroRNA-9 controls the expression of Granuphilin/Slp4 and the secretory response of insulin-producing cells. The Journal of biological chemistry. 2006; 281:26932–26942. [PubMed: 16831872]

Qu Q, Sun G, Li W, Yang S, Ye P, Zhao C, Yu RT, Gage FH, Evans RM, Shi Y. Orphan nuclear receptor TLX activates Wnt/beta-catenin signalling to stimulate neural stem cell proliferation and self-renewal. Nature cell biology. 2010; 12:31–40. sup pp 31–39. [PubMed: 20010817]

Risau W. Mechanisms of angiogenesis. Nature. 1997; 386:671–674. [PubMed: 9109485]

Ruhrberg C, Bautch VL. Neurovascular development and links to disease. Cellular and molecular life sciences: CMLS. 2013; 70:1675–1684. [PubMed: 23475065]

Ruhrberg C, Gerhardt H, Golding M, Watson R, Ioannidou S, Fujisawa H, Betsholtz C, Shima DT. Spatially restricted patterning cues provided by heparin-binding VEGF-A control blood vessel branching morphogenesis. Genes & development. 2002; 16:2684–2698. [PubMed: 12381667]

Sapkota D, Chintala H, Wu F, Fliesler SJ, Hu Z, Mu X. Onecut1 and Onecut2 redundantly regulate early retinal cell fates during development. Proceedings of the National Academy of Sciences of the United States of America. 2014; 111:E4086–4095. [PubMed: 25228773]

Schmidt R, Strahle U, Scholpp S. Neurogenesis in zebrafish - from embryo to adult. Neural development. 2013; 8:3. [PubMed: 23433260]

Scott A, Powner MB, Gandhi P, Clarkin C, Gutmann DH, Johnson RS, Ferrara N, Fruttiger M. Astrocyte-derived vascular endothelial growth factor stabilizes vessels in the developing retinal vasculature. PloS one. 2010; 5:e11863. [PubMed: 20686684]

Shi Y, Chichung Lie D, Taupin P, Nakashima K, Ray J, Yu RT, Gage FH, Evans RM. Expression and function of orphan nuclear receptor TLX in adult neural stem cells. Nature. 2004; 427:78–83. [PubMed: 14702088]

Shibata M, Nakao H, Kiyonari H, Abe T, Aizawa S. MicroRNA-9 regulates neurogenesis in mouse telencephalon by targeting multiple transcription factors. The Journal of neuroscience: the official journal of the Society for Neuroscience. 2011; 31:3407–3422. [PubMed: 21368052]

Shima DT, Gougos A, Miller JW, Tolentino M, Robinson G, Adamis AP, D'Amore PA. Cloning and mRNA expression of vascular endothelial growth factor in ischemic retinas of Macaca fascicularis. Investigative ophthalmology & visual science. 1996; 37:1334–1340. [PubMed: 8641836]

Stone J, Itin A, Alon T, Pe'er J, Gnessin H, Chan-Ling T, Keshet E. Development of retinal vasculature is mediated by hypoxia-induced vascular endothelial growth factor (VEGF) expression by neuroglia. The Journal of neuroscience: the official journal of the Society for Neuroscience. 1995; 15:4738–4747. [PubMed: 7623107]

Ulrich F, Ma LH, Baker RG, Torres-Vazquez J. Neurovascular development in the embryonic zebrafish hindbrain. Developmental biology. 2011; 357:134–151. [PubMed: 21745463]

Walchli T, Wacker A, Frei K, Regli L, Schwab ME, Hoerstrup SP, Gerhardt H, Engelhardt B. Wiring the Vascular Network with Neural Cues: A CNS Perspective. Neuron. 2015; 87:271–296. [PubMed: 26182414]

Wild R, Klems A, Takamiya M, Hayashi Y, Strahle U, Ando K, Mochizuki N, van Impel A, Schulte-Merker S, Krueger J, et al. Neuronal sFlt1 and Vegfaa determine venous sprouting and spinal cord vascularization. Nature communications. 2017; 8:13991.

Yu RT, Chiang MY, Tanabe T, Kobayashi M, Yasuda K, Evans RM, Umesono K. The orphan nuclear receptor Tlx regulates Pax2 and is essential for vision. Proceedings of the National Academy of Sciences of the United States of America. 2000; 97:2621–2625. [PubMed: 10706625]

Yuan J, Lei ZN, Wang X, Deng YJ, Chen DB. Interaction between Oc-1 and Lmx1a promotes ventral midbrain dopamine neural stem cells differentiation into dopamine neurons. Brain research. 2015; 1608:40–50. [PubMed: 25747864]

Zhang H, Qi M, Li S, Qi T, Mei H, Huang K, Zheng L, Tong Q. microRNA-9 targets matrix metalloproteinase 14 to inhibit invasion, metastasis, and angiogenesis of neuroblastoma cells. Molecular cancer therapeutics. 2012; 11:1454–1466. [PubMed: 22564723]

Zhang Y, Sloan SA, Clarke LE, Caneda C, Plaza CA, Blumenthal PD, Vogel H, Steinberg GK, Edwards MS, Li G, et al. Purification and Characterization of Progenitor and Mature Human Astrocytes Reveals Transcriptional and Functional Differences with Mouse. Neuron. 2016; 89:37–53. [PubMed: 26687838]

Zhao C, Sun G, Li S, Shi Y. A feedback regulatory loop involving microRNA-9 and nuclear receptor TLX in neural stem cell fate determination. Nature structural & molecular biology. 2009; 16:365–371.

Zhuang G, Wu X, Jiang Z, Kasman I, Yao J, Guan Y, Oeh J, Modrusan Z, Bais C, Sampath D, et al. Tumour-secreted miR-9 promotes endothelial cell migration and angiogenesis by activating the JAK-STAT pathway. The EMBO journal. 2012; 31:3513–3523. [PubMed: 22773185]

Highlights

- VEGF-A is expressed in human differentiated neurons prior to astrogenesis
- miR-9 is expressed in neural stem cells and negatively regulates neuronal VEGF-A
- miR-9-direct targets, *TLX* and *ONECUTs*, are transcriptional activators of *VEGF-A*
- miR-9 modulation of neuronal VEGF-A controls brain angiogenesis *in vivo*

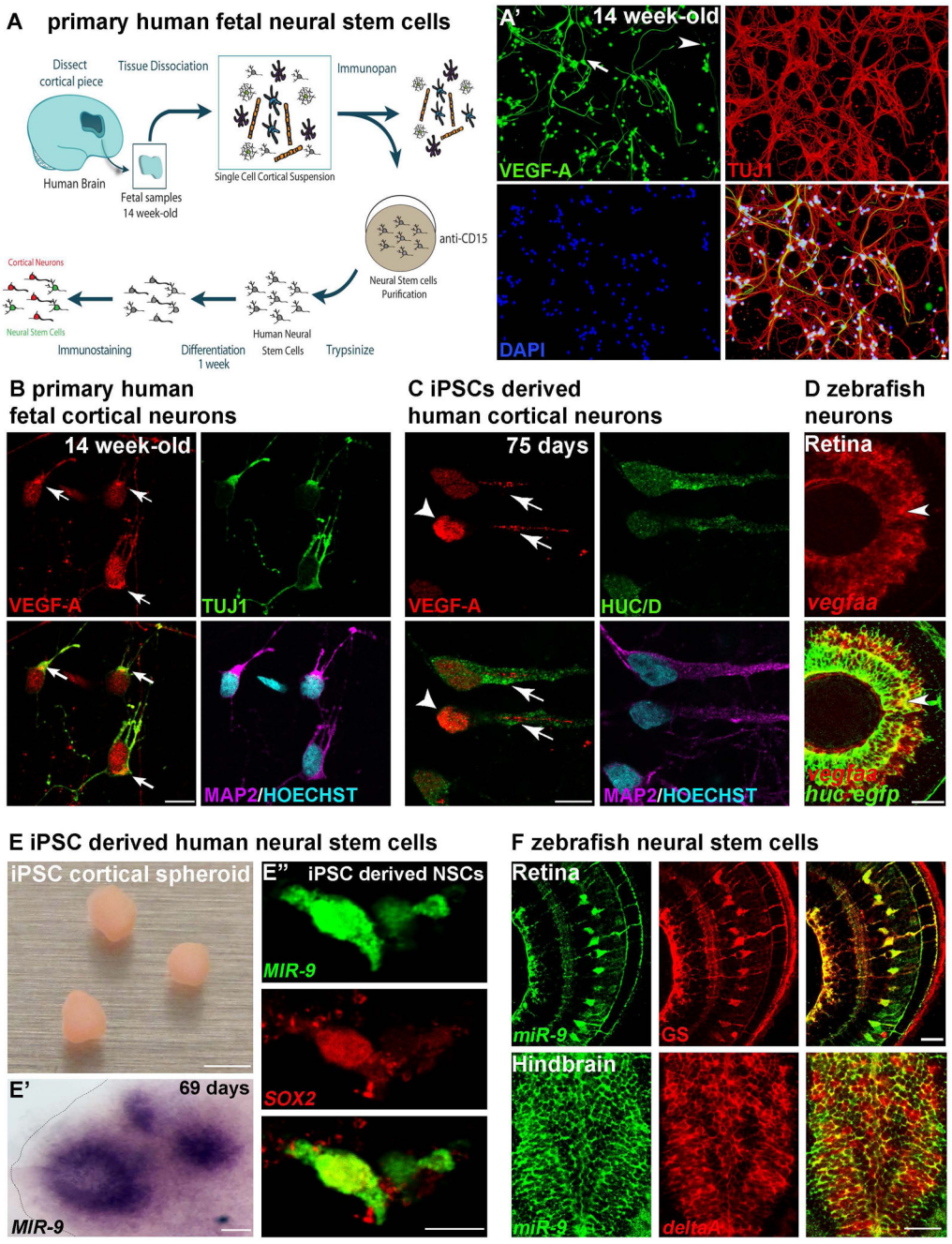

Figure 1. Neuronal VEGF-A and *miR-9* expression in NSCs are conserved in the human brain

(**A**) Schematic representation of the method used to obtain primary human neural stem cells form fetal brain at 14 weeks of development. At 7 days in culture (A′), a majority of the TUJ1 expressing embryonic neurons express detectable levels of VEGF-A (98.5%, n=201). NSCs (arrow) and neurons (arrowhead) express VEGF-A in primary human cell culture. **(B, C)** Confocal sections of primary human cortical neurons (B) and iPSCs-derived human cortical neurons (C) immunolabelled with VEGF-A. Young human cortical neurons show heterogeneous localization of VEGF-A (arrows show cytoplasmic and axonal localization, arrowhead indicates strong nuclear expression). **(D)** Confocal section of double in situ/

immunolabelling showing overlap in the expression of *vegfaa* and *Tg(huc:egfp)* post-mitotic neurons in the retina (arrowhead). (**E**) iPSC-derived human cortical spheroid in culture. *In situ hybridization* showing *MIR-9* expression in the ventricular-like zone of human cortical spheroid (E′). Confocal section of double *in situ* showing co-localization of *MIR-9* and *SOX2* in iPSC derived human NSCs (E″). (**F**) Confocal section of double immunolabelling with glutamine synthetase (GS) and EGFP in *Tg(hsa-MIR-9-2:egfp)* retina at 72 hpf, showing *miR-9* expression in retinal neural stem cells. Confocal section of double in situ/ immunolabelling showing overlap in the expression of *deltaA* and EGFP in *Tg(hsa-MIR-9-2:egfp)* hindbrain at 72 hpf. Dorsal view of the brain with anterior up. Lateral view of the retina. Scale bars: 25 μm (B, C), 100 μm (D, E′ and F), 4 mm (E) and 10 μm (A′ and E″).

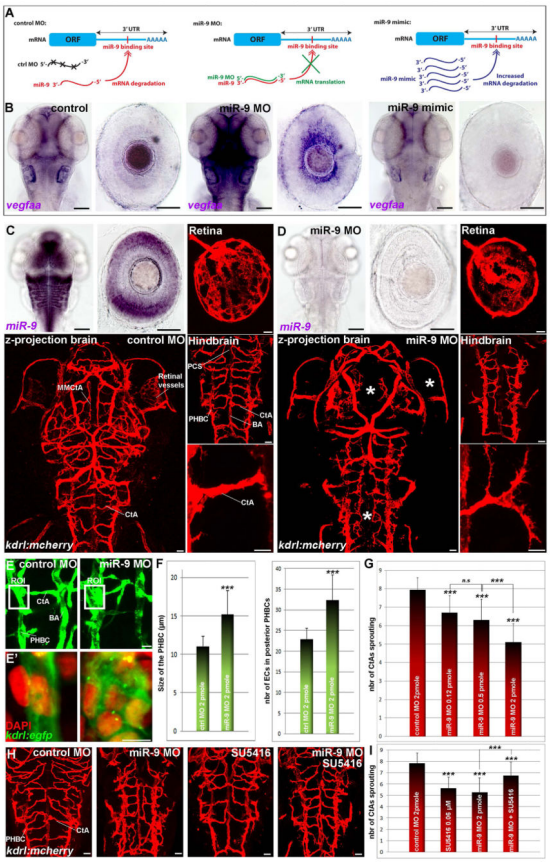

Figure 2. miR-9 controls brain vasculature development by limiting VEGF-A expression

(**A**) Schematic representation of the miR-9 MO and miR-9 RNA mimic effects. In presence of the miR-9 MO, miR-9 is paired with the MO, inhibiting the mRNA degradation. The miR-9 RNA mimic is ubiquitously expressed to allow the degradation of the miR-9 targets. (**B**) Whole-mount *in situ* hybridization against *vegfaa* in embryos at 48 hpf. *vegfaa* mRNA behaves like a miR-9 target showing an increase in the miR-9 knockdown and a decrease in the miR-9 gain of function. (**C, D**) Whole-mount in situ hybridization against *miR-9* shows that miR-9 knockdown does not affect brain and eye morphogenesis at 72 hpf. In miR-9 morphant *Tg(kdrl:mCherry)* brain at 72 hpf, the mesencephalic central artery (MMCtA), hindbrain and retinal blood vessels are affected (asterisk in D). In the hindbrain, Primordial Hindbrain Channels (PHBCs) are thicker and Central arteries (CtAs) are disorganized, thinner and show aberrant multidirectional sprouting. (**E**) Confocal projections of EGFP labelling in *Tg(kdrl:egfp)* at 72 hpf showing ECs (E′; EGFP+/DAPI+) in posterior PHBCs in control or miR-9 morphant larvae. (**F**) Quantification of the size of PHBC (µm) (ROI in E; control (n=33) or miR-9 MO (n=28)) and the total number of ECs recruited to form the posterior PHBCs (control (n=12) or miR-9 MO (n=10)) at 72 hpf. **(G)** Quantification of the number of CtAs found on each hemi-hindbrain in the control (n=20) or the miR-9 MO dilution series (n=34, 28 and 56 for croissant dilutions respectively) at 72 hpf. **(H, I)** *Tg(kdrl:mCherry)* brain at 72 hpf showing blood vessel formation in the hindbrain (H), and quantification of the number of CtAs found on each hemi-hindbrain (I), of control (n=40), 0.06 µM SU5416 treated (n=48), miR-9 morphant (n=48), and miR-9 MO treated with 0.06

μM SU5416 (n=30) larvae. Dorsal view of the brain with anterior up. Lateral view of the retina. Scale bars: 100 μm for ISH in B–D and 10 μm (C–E′ and H). Error bars represent s.d. *P<0.05, **P<0.001, ***P<0.0005, determined by t-test, two-tailed.

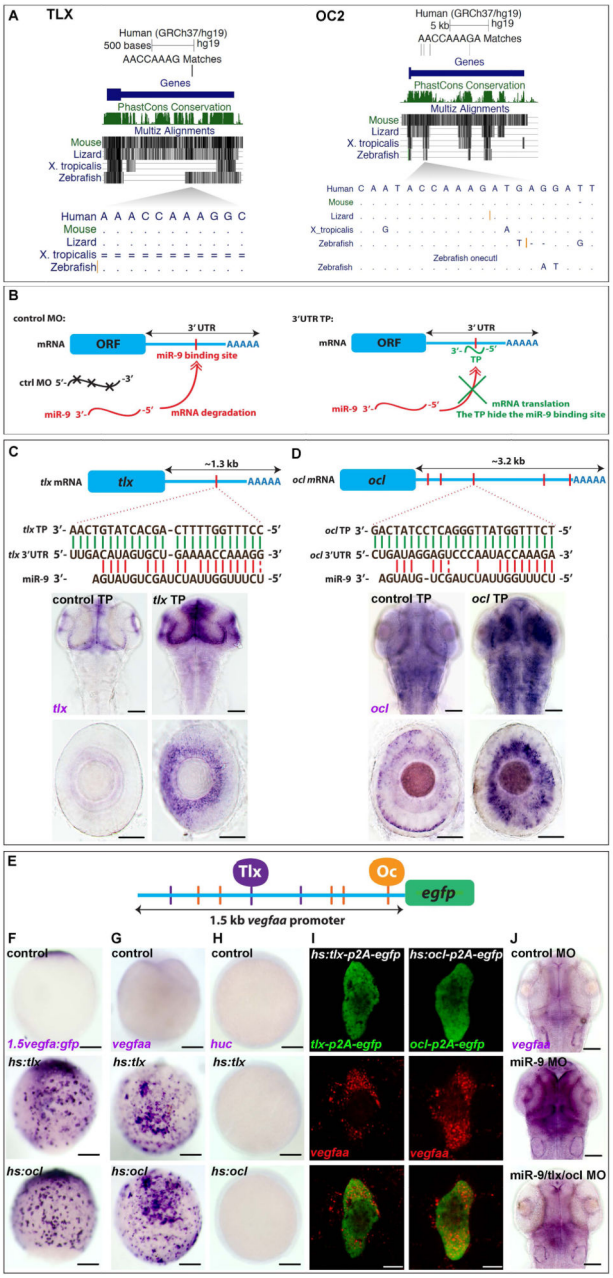

Figure 3. *tlx* and *onecut* are direct miR-9 targets regulating *VEGF-A* transcriptional expression *in vivo*

(A) Alignments of vertebrate TLX and ONECUT2 orthologues show strong conservation in the 3′UTR containing a putative miR-9 binding site. (**B**) Schematic representation of the TP assay. In the presence of the TP, the miR-9 binding site is not accessible and the mRNA degradation is inhibited. **(C-D)** Schematic representation of the zebrafish *tlx* (C) and *ocl* (D) mRNA indicating the sequence of the putative miR-9 binding site in the 3′UTR (red) and the alignment with miR-9 or TP. *tlx* and *ocl* mRNA behave like direct miR-9 targets showing an increase in the TP context. **(E)** Schematic representation highlighting putative Tlx (NAGTCA/purple; (Qu et al., 2010; Yu et al., 2000)) and Onecut (NN(A/G)TC(A/C)A(T/

G)NN/orange; (Lannoy et al., 1998; Plaisance et al., 2006)) binding sites in 1.5kb of the *vegfaa* promoter. **(F)** Whole-mount *in situ* hybridization against *egfp* driven by 1.5kb of the *vegfaa* promoter. Embryos were injected with *vegfaa:egfp* only, *hs:tlx,* or *hs:ocl* and heat-shocked at 7 hpf. Embryos display ectopic expression of the *egfp* mRNA 2 hours after treatment showing that Tlx and Onecut have the ability to induce the transcription via 1.5kb of the *vegfaa* promoter. **(G, H)** Whole-mount *in situ* hybridization against *vegfaa* and *huc* in embryos at 9 hpf. Embryos were injected with *hs:tlx* or *hs:ocl* and heat-shocked at 7 hpf. Embryos display ectopic expression of *vegfaa*, but not *huc*, two hours after treatment, showing that Tlx and Onecut transcriptions factors have the ability to induce the transcription of the endogenous *vegfaa* gene independently of the neuronal fate. **(I)** Mosaic expression of Tlx-p2A-EGFP or Ocl-p2A-EGFP by heat-shock at 8.5 hpf induce endogenous *vegfaa* expression in as little as 30 min in a cell autonomous manner suggesting a direct regulation. **(J)** Whole-mount *in situ* hybridization against *vegfaa* in embryos at 48 hpf injected with the control MO, miR-9 MO, or miR-9 MO with *tlx* and *ocl* MOs. Dorsal view, Anterior up. Lateral view of the retina. Scale bars: 100 μm (C, D, F–H and J) or 10 μm (I).

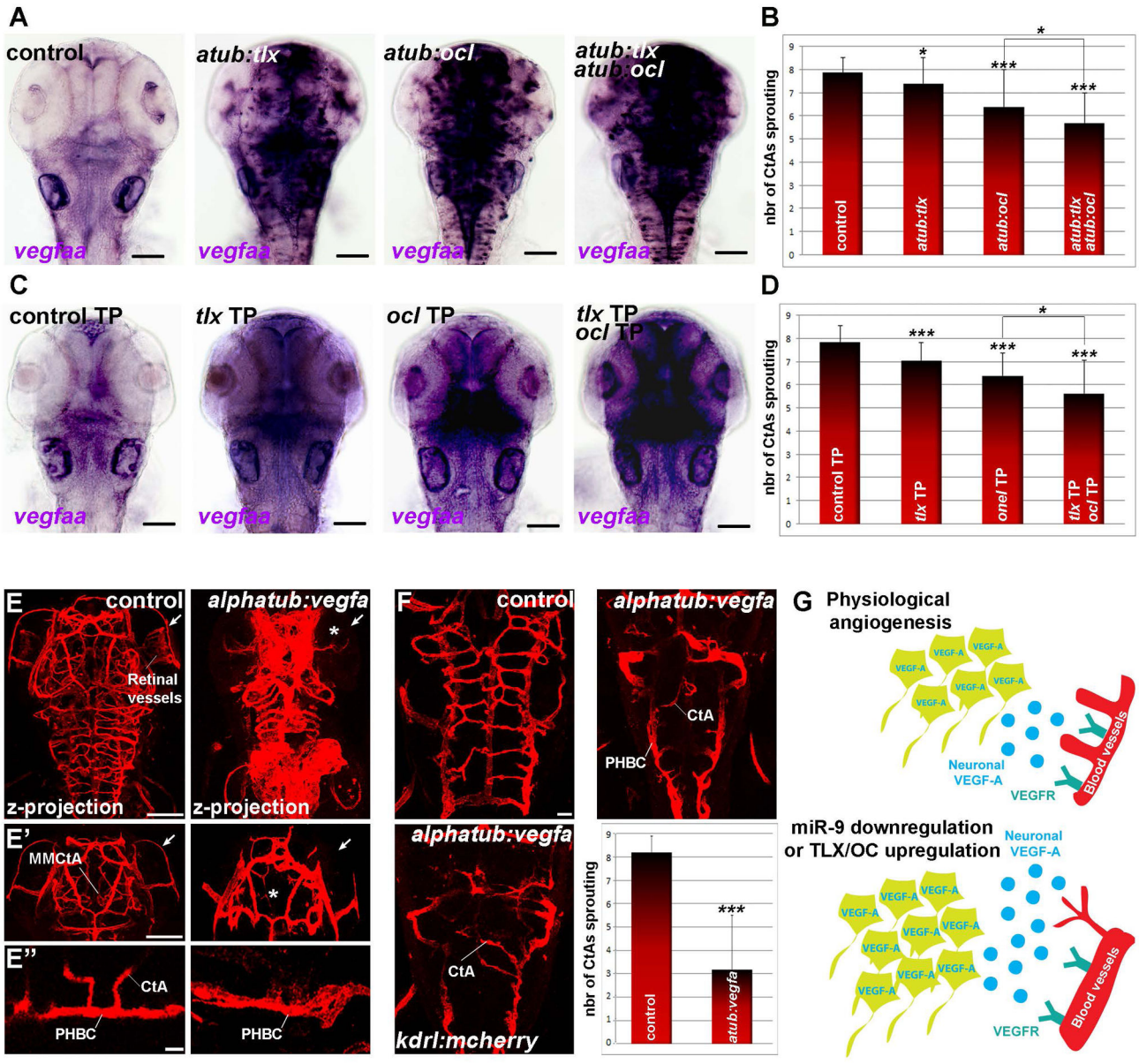

Figure 4. Tlx and Oc dependent neuronal expression of VEGF-A affect brain vasculature development

(A) Whole-mount *in situ* hybridization against *vegfaa* at 48 hpf in controls or embryos expressing *uas:tlx*, *uas:ocl,* or *uas:tlx* and *uas:ocl* in a pan-neuronal manner in *Tg(alpha-tubulin:gal4)*. **(B)** Quantification of the number of CtAs found on each hemi-hindbrain in controls (n=34) or larvae expressing *uas:tlx* (n=46), *uas:ocl* (n=46) or *uas:tlx* and *uas:ocl* (n=46) in a pan-neuronal manner in *Tg(alpha-tubulin:gal4)* at 72 hpf. **(C)** Whole-mount *in situ* hybridization against *vegfaa* in embryos at 48 hpf injected with the control MO, *tlx* TP, *ocl* TP, or *tlx* and *ocl* TP. **(D)** Quantification of the number of CtAs found on each hemi-hindbrain in the control MO (n=32), *tlx* TP (n=34), *ocl* TP (n=34), or *tlx* and *ocl* TP (n=34) larvae at 72 hpf. (**E**) Neuronal expression of VEGF-A in the *Tg(alpha-tubulin:gal4)* line leads to a global increase in ECs and/or blood vessels formation in the brain at 72 hpf. While

most of the vessels appear to be thicker, the mesencephalic central artery (MMCtA) and retinal blood vessels are reduced or missing (arrow and asterisk in E and E′). In the hindbrain, PHBCs are thicker while CtAs sprouting is reduced, suggesting that their development is affected following neuronal VEGF-A expression (E″). (**F**) Quantification of the number of CtAs found on each hemi-hindbrain in controls (n=30) and larvae expressing *vegfaa* (n=20) in neurons at 72 hpf (F). **(G)** During the normal development of the neurovascular system, miR-9 represses the expression of Tlx and Oc to limit the level of neuronally-derived VEGF-A. A reduction of miR-9 expression and/or an overexpression of Tlx/Oc increase the level of neuronal VEGF-A and affects the development of the brain vasculature. Dorsal view of the brain with anterior up. Scale bars: 100 μm (A, C, E and E′) or 10 μm (F and E″). Error bars represent s.d. *P<0.05, **P<0.001, ***P<0.0005, determined by t-test, two-tailed.